coatings

Article

Biostable Fluorine-Containing Coatings on the Surface of Polymers

Fedor Doronin [1,*], Georgy Rytikov [2], Andrey Evdokimov [1], Yury Rudyak [1], Mikhail Savel'ev [1] and Victor Nazarov [1]

[1] Faculty of Printing Industry, Moscow Polytechnic University, 107023 Moscow, Russia
[2] Department of Information Systems, State University of Management, 109542 Moscow, Russia
* Correspondence: f.a.doronin@mospolytech.ru

Abstract: We considered the formation of the integrated biostable coating on the surface of several polymers using the original gas-phase fluorination technology. The effectiveness of surface modification of low-density polyethylene (LDPE) and polypropylene (PP) was confirmed by corresponding changes in the absorption spectra of infrared radiation with the modified samples. The gas-phase fluorination quality of ultrahigh molecular weight polyethylene (UHMWPE) and nitrile butadiene rubber (NBR) surfaces was evidenced by the results of scanning electron microscopy (SEM) and energy dispersion analysis (EDS). As was shown with the direct measurements of water and ethyleneglycol wetting angles, the properties differences of the polymer materials with modified surfaces from the initial one correlated well with the change in free surface energy induced by the chemical and morphological transformations under the fluorine and oxygen-containing gas mixtures treatment. The developed technique for the bio-contamination degree quantifying, based on the computer analysis of the corresponding images, allowed us to establish that gas-phase fluorination of the surface approximately doubles the time during which the biofouling of LDPE, PP and UHMWPE with the mixed colony of Rivularia and Stigonema Minutum algae occurs under natural conditions. No positive effect from fluorination was observed for NBR, which was explained, from our point of view, by the difference in the mechanisms of biostability for the considered polymer materials.

Keywords: microalgae; biostability; fluorination; thermoplastics; elastomers; mathematical modeling

check for updates

Citation: Doronin, F.; Rytikov, G.; Evdokimov, A.; Rudyak, Y.; Savel'ev, M.; Nazarov, V. Biostable Fluorine-Containing Coatings on the Surface of Polymers. *Coatings* **2023**, *13*, 424. https://doi.org/10.3390/coatings13020424

Academic Editor: Liqun Xu

Received: 9 December 2022
Revised: 5 February 2023
Accepted: 9 February 2023
Published: 13 February 2023

Copyright: © 2023 by the authors. Licensee MDPI, Basel, Switzerland. This article is an open access article distributed under the terms and conditions of the Creative Commons Attribution (CC BY) license (https://creativecommons.org/licenses/by/4.0/).

1. Introduction

When using polymers in static and moving elements of technical systems and equipment operating in extreme conditions, it is necessary to ensure reliable sealing and increase the service life, since uncontrolled changes in the operational properties of products made from thermoplastics and elastomers can lead to emergency situations [1]. One of the problems with the reliability of hermetic units made of polymers is their low bioresistance to various microorganisms and microalgae, which are highly adaptable to environmental changes, which creates the risk of more aggressive strains of micromycetes [2–4]. To solve the problem of biodegradation of polymers, the following are used: (a) biocides [5–8], intended for the destruction of degrading microorganisms, the colonies of which could develop on a particular polymer-based product; (b) anti-adhesive (bio-insulating) coatings that prevent the development of colonies of degrading microorganisms on the surface of polymers and products based on them [9–12]. Fluorinated polymers have high chemical resistance, mainly due to the peculiarities of their chemical structure and morphology [13]. Taking into account that the mechanisms of biological destruction are mainly associated with the local chemical and micromechanical action of microbial colonies on the surface layers of the destructible material [14], it seems relevant to use technologies for the formation of protective nanoscale biostable integrated coatings [15]. A promising method for transforming the surface and physicochemical characteristics of polymers are the methods of gas-phase fluorination [16] and oxyfluorination [17], which allows forming an integrated

fluorine- and oxygen-containing layer on their surface, providing targeted control over a wide range of wetting [18], adhesion [19], wear resistance [20], biostability [21] and other functional properties. The development of multifunctional materials with antimicrobial coating for biomedical applications is comprehensively described in [22].

The positive effect of fluorination to impart antimicrobial properties on dental composites and nonwoven fabrics was demonstrated in [15,23]. The created chemically stable fluorine-containing hydrophobic layer significantly reduced the growth degree of the bacteria (*Staphylococcus aureus*, *Escherichia coli*, *Candida albicans*) mixed colony on the polypropylene fibers' surfaces, which, in particular, indicates the adhesive mechanism of microorganisms fixing on the polymer materials' surface.

This hypothesis was also confirmed in [24] when studying the resistance of fluorinated ethylene propylene (FEP) to *S. aureus* and *R. aeruginosa*.

At the same time, the less studied influence of fluorination on the polymer bioresistance to microalgae is not only of fundamental but also of applied interest.

The purpose of this work is to study the biostability of the initial and fluorinated polymers to the microalgae (*Rivularia* and *Stigonema minutum*) mixed colony impact in vivo.

2. Materials and Methods

The experimental samples of our research were: ultra-high molecular weight polyethylene (UHMWPE), low-density polyethylene (LDPE), polypropylene (PP), nitrile butadiene rubber (NBR). The surface modification of polymers was performed by direct fluorination [13,25] with a gas mixture of 15%F_2/0.5%O_2/82.5% for 180 min in a stainless-steel reactor [26] (Figure 1).

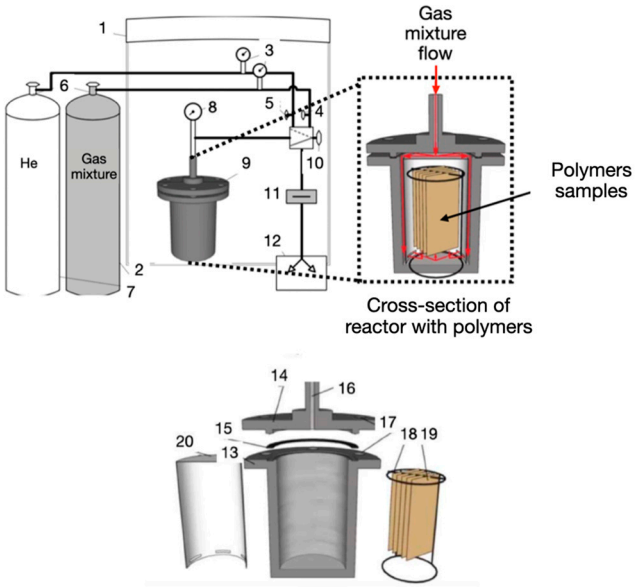


Figure 1. The laboratory equipment of direct gas phase fluorination and oxyfluorination of polymers [26]. (1 is air extractor, 2 is cylinder with a modifier, 3 is corrosion-resistant pressure gauges, 4 and 5 is stainless steel needle valves, 6 is cylinder valves, 7 is cylinder with helium, 8 is corrosion-resistant manovacuummeter, 9 is stainless steel reactor, 10 is shut-off valve, 11 is chemical absorber, 12 is vacuum pump, 13 is housing, 14 is lid, 15 is sealing ring, 16 is fitting, 17 is holes for bolted connection, 18 is wire bracket, 19 is samples of polymers, and 20 is gas mixture flow distributor).

The direct fluorination process was carried out in three stages [26]: the preparation of polymers (wiping LDPE, PP, NBR and UHMWPE with ethylalcohol to remove possible contaminants and the degassing of polymers by vacuuming), the gas-phase fluorination and the reaction products were removed from the reactor by vacuuming and using chemical absorbers.

A layered structure (Figure 2) was formed as a result of gas-phase surface fluorination: the surface layer had a fairly homogeneous chemical composition close to fluoropolymers; the modification degrees of different transient zone fragments significantly differed from each other (from "unmodified" to " wholly fluorinated" regions); the chemomorphological transformations of the initial polymer matrix were not observed at a depth of more than 2 microns.

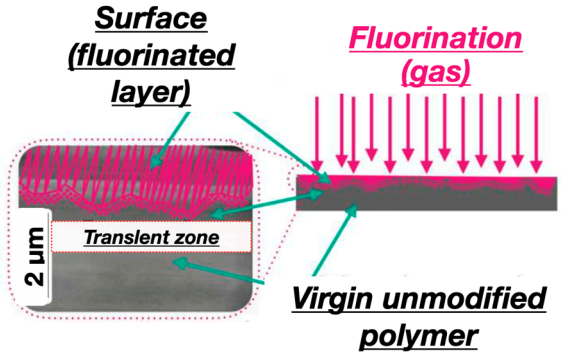


Figure 2. The schematic structure of the fluorinated polymer surface layers.

The study of the surface structure of the experimental samples before and after fluorination was carried out using a high-resolution auto-emission scanning electron microscope (JSM-7500 FA (JEOL, Tokyo, Japan)). The corresponding changes in chemical composition were determined using the IR-Fourier spectroscopy technique (FT-801 IR-Fourier spectrometer (Simex, Nizhny, Russia)). The study of the biostability of the experimental samples of algae Rivularia, StigonemaMinutum was carried out for 47 days in a container (steel barrel) under natural sunlight conditions (in the "day-night" mode—at the latitude of Moscow) at a temperature of 30 ± 7 °C. The samples were fixed on a steel grid and placed in a steel barrel filled with river water (Figure 3).

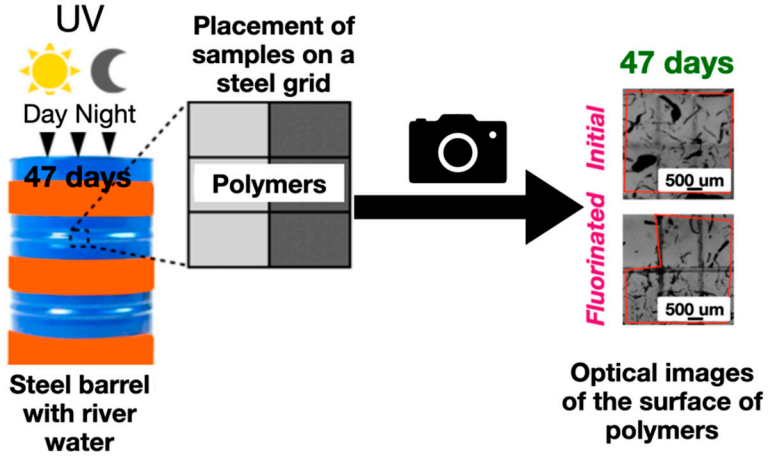


Figure 3. Study of the biostability of the initial and fluorinated polymers in microalgae colonies (Rivularia, StigonemaMinutum, etc.) during 47 days. The samples were fixed on a stainless steel grid.

During the 47 days of testing, the samples were photographed with a digital camera, Nikon D90 (Nikon Inc., Tokyo, Japan), using a tripod.

The digital sample's surface optical image is a tabular dependence $L(x,y)$ of pixel lightness L on its coordinates (x,y). When studying a set of corresponding optical images, it is convenient [27] to determine, for each pixel position (x,y), the statistical characteristics:

$$\overline{L}(x,y) = \frac{1}{N} \cdot \sum_{k=1}^{N} L_k(x,y) \quad (1)$$

$$\sigma_L(x,y) = \sqrt{\frac{1}{N-1} \cdot \sum_{k=1}^{N} \left(L_k(x,y) - \overline{L}(x,y)\right)^2} \quad (2)$$

$$V_L(x,y) = \sigma_L(x,y)/\overline{L}(x,y) \quad (3)$$

where the horizontal line above L means the arithmetic averaging procedure, σ_L and V_L are the absolute and the relative standard deviations, respectively.

The quantitative analysis of the experimental samples' algae fouling degree was based on the computer processing of the corresponding surface images. Since the algae contamination was visually observed a few days after the start of the experiment, we decided to use the degree of optical image heterogeneity as an indicator of the biostability of the polymer materials under consideration.

We applied the original technique (including the synthesis of variational-rotational patterns and the statistical processing of pixel lightness) of dispersion analysis to quantify the biofouling optical heterogeneity of the surface images of the experimental samples.

Each variation-rotation pattern was the result of pixel-by-pixel averaging of a series of digital clones formed by fixed angles planar rotation of the initial sample's surface image.

The rotated copies of the initial image were created using the well-known equations

$$\begin{cases} \widetilde{x}_k = x \cdot \cos(\varphi_k) + y \cdot \sin(\varphi_k) \\ \widetilde{y}_k = -x \cdot \sin(\varphi_k) + y \cdot \cos(\varphi_k) \end{cases} \quad (4)$$

and the assignment operation $\widetilde{L}_k(x,y) = L(\widetilde{x}_k, \widetilde{y}_k)$.

Here, $L(x,y)$ is a digital image of the surface of the experimental sample; $\left\{\widetilde{L}_k(x,y)\right\}_9$ is a set of nine cloned images in the corresponding coordinate systems $((\widetilde{x}_k, \widetilde{y}_k))$ rotated at φ_k angles.

In order to demonstrate the sensitivity of the method, a number of calibration tests were performed [27]. As a simulation model, we used the uniformly distributed random numbers (Figure 4A) with $\overline{L} = 108$ and $\sigma_L = 16$. The variation rotational pattern for the real SEM-image with the same $\overline{L} = 108$ and $\sigma_L = 16$ is represented in (Figure 4B).

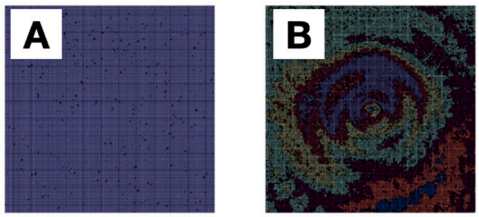


Figure 4. Variational-rotational patterns characterizing morphologically homo- (**A**) and heterogenic (**B**) surfaces Reprinted with permission from [27].

Therefore, the variational-rotational approach can effectively characterize the surface morphology, which determines some functional properties of the polymer surface (biostability, wetting, adhesion, friction coefficient).

3. Results and Discussion

The visual analysis of the initial and the oxyfluorinated LDPE samples surface SEM images (Figure 5) made it possible to assess the dependence of the observed morphology changes on the fluorine and oxygen concentrations in the modifying gas mixture [27]. They were caused by both (a) the transformations of chemical composition and structure of the material's near-surface layers (confirmed by means of IR Fourier spectroscopy (Figure 6) and point EDS-analysis (Figure 7)), as well as (b) the differences in the kinetics of the amorphous and the crystalline surface regions modification processes.

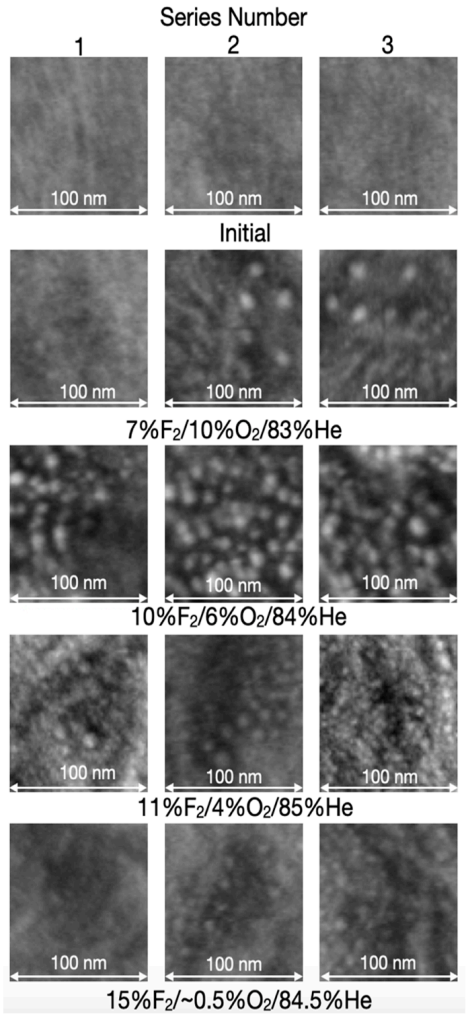


Figure 5. The SEM images of the oxyfluorinated LDPE samples (the characteristic size (square side) of the analyzed regions ~ 100 nm) [28].

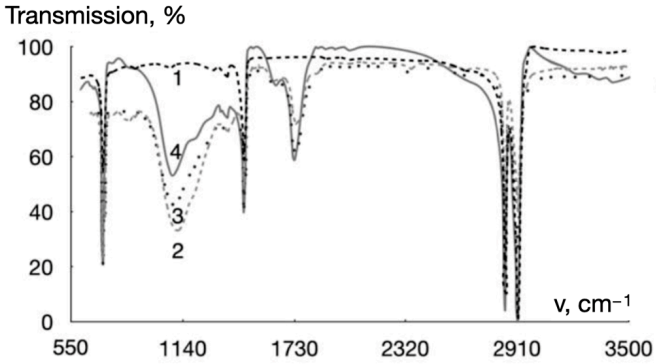


Figure 6. IR spectra of LDPE depending on the ratio of the components of the gas mixture ($F_2/O_2/He$) with a modification duration of 180 min: initial (1) 15/0.5/84.5 (2) 10/6/84 (3) and 7.5/10/82.5 (4).

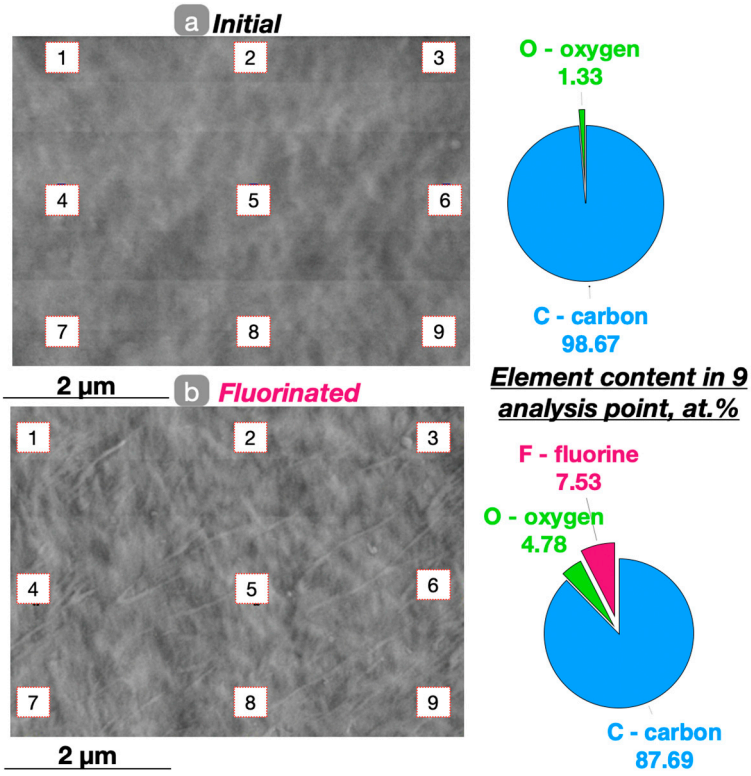


Figure 7. EDS analysis of the surface of LDPE (**a**) initial (**b**) fluorinated by gas mixture (F_2/O_2/He) 15/0.5/84.5 for 180 min. (1−9 is analysis point).

The wide absorption lines appear in the IR spectrum of LDPE as a result of the fluorine- and oxygen-containing gas mixtures treatment. We associate them with the formation of C-F bonds from monofluorosubstituted to perfluorinated compounds (800–1300 cm^{-1}), and due to the formation of oxygen-containing groups of various types, for example, –COF and –COOH (1700–1800 cm^{-1}).

The presence of the fluorine (4.8 ± 0.5 at. %) and the oxygen (7.5 ± 0.8 at. %), as well as the uniformity of their distribution over the surface layer of the modified polymer material are confirmed by the results of point EDS analysis (Figure 7).

The creation of a fluorine-containing layer in LDPE is also confirmed by EDS-spectroscopy in Figure 8 and Table 1 [29].

In the initial materials, the contributions of non-functionalized sp2 and sp3 C atoms occur at lower binding energies (BE). The asymmetric shoulder toward higher BEs could correspond to surface defects, C–H and C–O groups. After fluorination, the position of the components relative to nonfluorinated C atoms remains unchanged, but other numerous contributions occur at higher BEs [29].

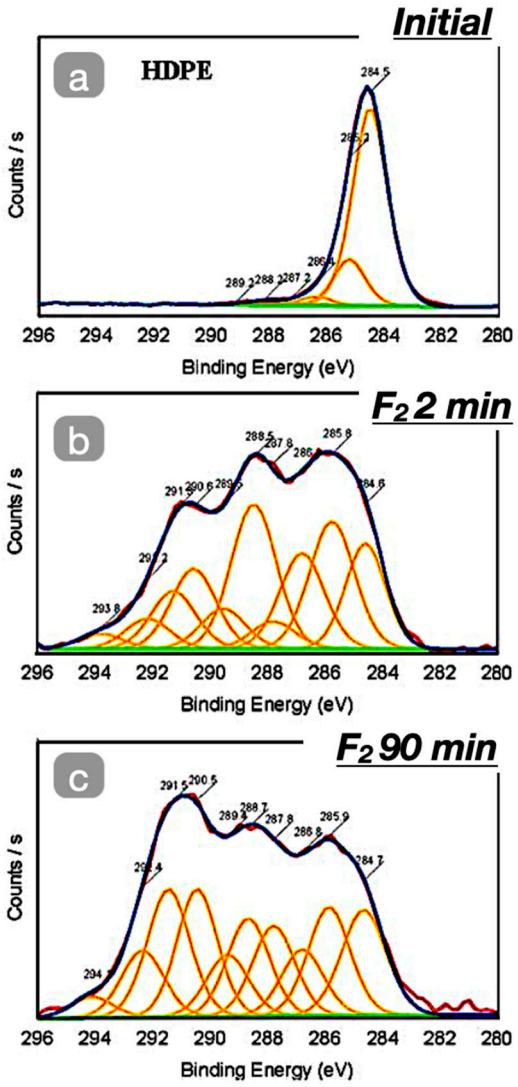


Figure 8. Fitted C1s EDS spectra of initial (**a**) and fluorinated LDPE samples (treatment duration was equal to 2 (**b**) and 90 (**c**) min) [29].

Table 1. Assignment of the XPS C1s components [29].

Chemical Bond	Shift (eV) Relative to the CHn Component at 284.5 eV
CHn	-
CH2–CHF	0.7–1.1
CH2–CF2	2.0
CHF–CH2	-
CHF–CHF	3.0–3.5
CHF–CF2	4.5
CFx–CF–CFx′ (x, x′ = 2, 3)	-
CF2–CH2	5.3–5.5
CF2–CHF	6.2–6.8
CF2–CF2	7.8
CF3–CFx	9.1

Obviously, the chemical-morphological transformation of LDPE as a result of modification leads to a change in the hydrophilic-hydrophobic balance of the corresponding surfaces, which is confirmed by the differences in the wetting angles of distilled water and

ethylene glycol, as well as the values of free surface energy depending on the composition of gas fluoro-oxygen-containing mixtures (Table 2).

Table 2. The edge wetting angles for the LDPE substrates oxyfluorinated under the various modification modes [28].

Surface Parameters			Gas Mixture Components, Vol.%		
Free Surface Energy, mJ/m^2	**Θ_w, °**	**Θ_e, °**	**He**	**F_2**	**O_2**
27 ± 3	78 ± 8	63 ± 6	-	-	-
46 ± 5	54 ± 5	22 ± 2	83 ± 1	7.0 ± 0.5	10.0 ± 0.5
44 ± 4	57 ± 6	28 ± 3	84 ± 1	10.0 ± 0.5	6.0 ± 0.5
46 ± 5	54 ± 5	32 ± 3	85 ± 1	11.0 ± 0.5	4.0 ± 0.5
41 ± 4	67 ± 7	34 ± 3	84.5 ± 0.5	15.0 ± 0.5	0.5 ± 0.5

The biostability of the considered polymers is determined by the chemical structure and nanotexture of their surface and, most likely, by the free surface energy and, as a consequence, by the amount of primary adhesion of microalgae.

Due to the optical properties of LDPE (Figure 9A), PP (Figure 9B), the transparency of experimental samples was observed at the initial stages of the survey, and, during the exposure to microalgae, its gradual decrease was recorded due to bioadhesion and biofouling of the polymer surface by algae fractions. Microalgae began to adhere to polymer surfaces mainly on the fourteenth day and only after microscopic algae fractions formed a kind of coating for them, providing, apparently, the possibility of their mechanical attachment and/or nutrition. Moreover, the number of adherent microalgae is determined, among other things, by the transformation of the polymer surface morphology due to the long time spent in water at a temperature of ~30 °C under periodic exposure to UV radiation ("day-night").Visually, using the examples of LDPE (Figure 9A) and UHMWPE (Figure 9D), it can be seen that the biofouling rate of fluorinated polymers is significantly lower than that of untreated ones, which is due to the presence of a more developed surface morphology and a uniform fluoroplast-like barrier layer on the polymer surface, which is verified by the results of IR-spectroscopy and EDS analysis [18–21]. The barrier effect is less pronounced due to the more labile surface structure for NBR (Figure 9C).

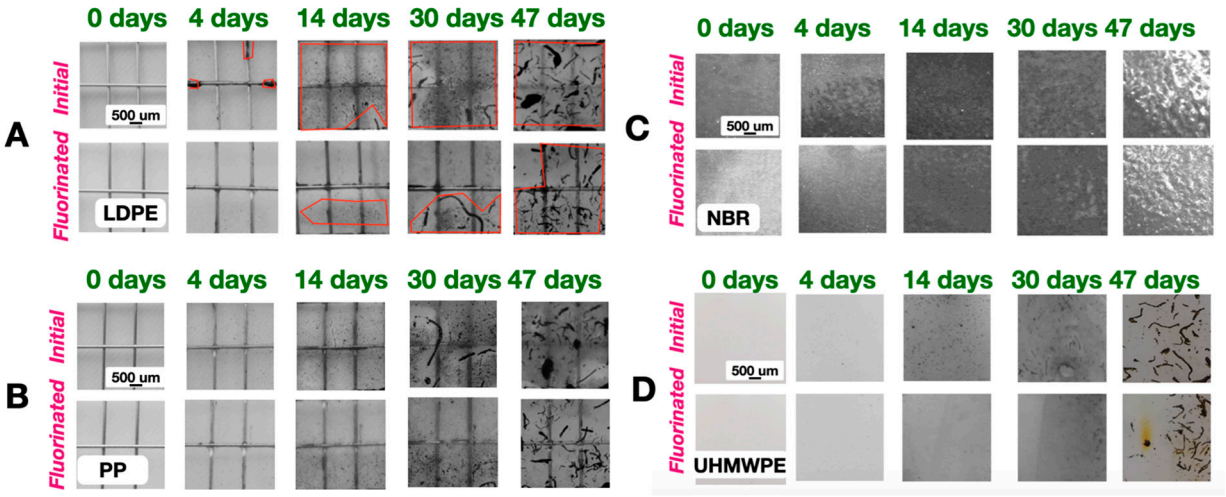


Figure 9. The effect of microalgae on the initial and fluorinated (gas mixture of 15%F2/0.5%O2/82.5%) LDPE (**A**), PP (**B**), NBR (**C**), UHMWPE (**D**) for 47 days. The red lines show the areas affected by algae.

In order to provide the possibility of objectivization, formalization and, in the future, automation of the procedure for studying polymers for biostability, the concept of

variational-rotational analysis of optical images of polymers before and after biodegradation was applied. To obtain a variational-rotational pattern based on the optical image of the polymer, digital images were formed, rotated relative to the original at angles of 10, 20, 30, 40, 50, 60, 70, 80 and 90 degrees (if necessary, the rotational sampling step could be arbitrarily chosen). For each pixel of the variation-rotation pattern, the mean value, standard deviation and brightness variation coefficient were calculated. As a quantitative measure of the degree of biocontamination of the polymer surface, we use the optical heterogeneity of its image. To assess optical heterogeneity, we used the mean value, standard deviation and the maximum value of the variation coefficient over the entire variation-rotational pattern. An increase in the standard deviation value of the pixel brightness variation coefficient indicated an increase in the area of biocontamination. An increase in the maximum value indicated an increase in the contrast of the image associated with local features of the thickness distribution of "biocoatings" formed by microalgae on the surface of the experimental samples. The dependences of the discussed values on the duration of the exposure to biodestructors for PP are presented in Tables 3 and 4.

Table 3. The effect of microalgae on the initial PP.

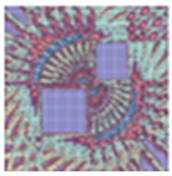
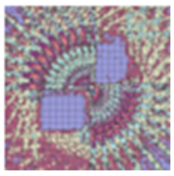
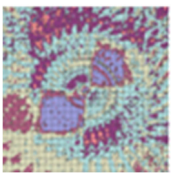
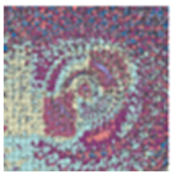
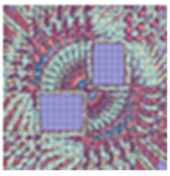
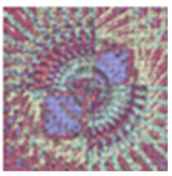
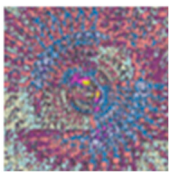
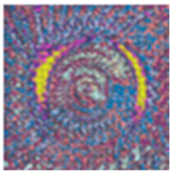
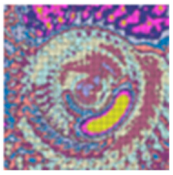
Duration, Days	**0**	**4**	**14**	**30**	**47**
Variational-rotational patterns (analysis of Figure 9B)					
$\overline{V}_{B_{ij}}$	0.150	0.121	0.151	0.195	0.313
σ_V	0.087	0.066	0.057	0.073	0.126
$\max\left(V_{B_{ij}}\right)$	0.582	0.391	0.395	0.586	0.862

Table 4. The effect of microalgae on the fluorinated PP.

Duration, Days	**0**	**4**	**14**	**30**	**47**
Variational-rotational patterns (analysis of Figure 9B)					
$\overline{V}_{B_{ij}}$	0.154	0.125	0.247	0.308	0.246
σ_V	0.080	0.062	0.085	0.103	0.133
$\max\left(V_{B_{ij}}\right)$	0.539	0.442	0.714	0.871	0.693

It has been established that the fluorination of PP contributes to a decrease in the rate of microalgae biofouling, which is due to a decrease (Figure 9B) in the adhesion of microalgae at the initial stage (14 days), which may be a consequence of an increase in the characteristic size of textural inhomogeneities as a result of surface modification of polyolefins (Figure 5). At the same time, when microalgae act on PP for more than 30 days, the active development of microalgae colonies is observed, comparable with the nature of the effect on the original PP. The kinetics of biofouling of the initial and fluorinated NBR samples radically differ from those observed for PP: the initial NBR practically ceases to grow microalgae after 4 days in the water, while the fluorinated one undergoes more efficient destruction.

The observed slight increase in the optical heterogeneity of the images of the initial NBR (Table 5) is probably due to the partial swelling of the rubber in water. A similar effect is observed for the fluorinated NBR (Table 6), but the decisive contribution to the optical heterogeneity is made by small-sized algae that attach to the surface, although they are not capable of forming a large-sized colony. Apparently, the mechanism of the biostability of elastomers is due not to the prevention of bioadhesion, but to the biocidal action of substances that are gradually extracted into the water during the swelling of rubber. Then, the biofouling of fluorinated samples is associated with the barrier properties of the surface layer, which prevents the migration of the rubber compounds ingredients and is desorbed after fluorination HF into water. Thus, gas phase fluorination of thermoplastics reduces the bioadhesion rate of microalgae in the natural environment, but does not make it possible to stop the biocontamination of the protected surfaces. At the same time, the fluorination of elastomers prevents the migration of ingredients with a biocidal effect of the polymer volume into water, so the biocontamination of the modified surfaces slightly increases.

Table 5. The effect of microalgae on the initial NBR.

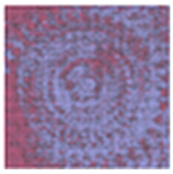
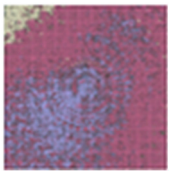
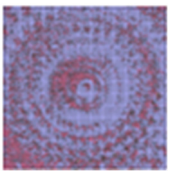
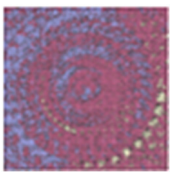
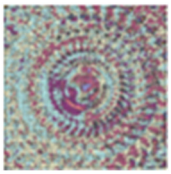
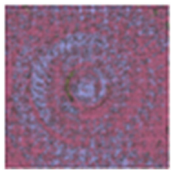
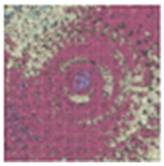
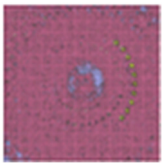
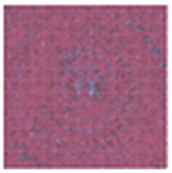
Duration, Days	**0**	**4**	**14**	**30**	**47**
Variational-rotational patterns (analysis of Figure 9C)					
$\overline{V}_{B_{ij}}$	0.046	0.059	0.039	0.058	0.150
σ_V	0.014	0.021	0.022	0.028	0.061
$\max\left(V_{B_{ij}}\right)$	0.317	0.329	0.451	0.829	1.053

Table 6. The effect of microalgae on the fluorinated NBR.

Duration, Days	**0**	**4**	**14**	**30**	**47**
Variational-rotational patterns (analysis of Figure 9C)					
$\overline{V}_{B_{ij}}$	0.056	0.093	0.065	0.063	0.168
σ_V	0.053	0.050	0.061	0.018	0.057
$\max\left(V_{B_{ij}}\right)$	1.452	1.605	1.352	0.272	0.364

4. Conclusions

We developed a new based on the computer image analysis approach to the quantification of the polymer material bio-contamination degree. It allowed us to perform a comparative study of bio-adhesion resistance for the algae (Rivularia and StigonemaMinutum) mixed colony growth on the surfaces of the initial and the fluorinated polymer samples. The formation of integrated thin-film coatings on the surfaces of LDPE, UHMWPE, PP and NBR was carried out using the original gas-phase surface fluorination technique. The effectiveness of the modifying gas mixture (85 vol.% helium and 15 vol.% fluorine) on the polymer surface layers was confirmed by using IR-Fourier spectroscopy and EDS analysis. The transformations of morphology and the distribution of chemical elements on the surface of modified polymer materials were evidenced by the presented results of

the scanning electron microscopy. For the LDPE, UHMWPE and PP samples, fluorination led to a decrease in the fouling rate; whereas, for NBR, it led to an increase. We explain this by the biocidal properties of the ingredients extracted by unmodified NBR samples into the environment and the formation of a barrier layer as a result of fluorination that prevents this phenomenon. Therefore, the gas phase fluorination of the vast majority of polymers leads to an increase in their biostability, but in some cases it can also lead to an acceleration of bio-growth in a natural aquatic environment. In the near future, we plan to establish the nature and the degree of degradation of the produced bio-resistant integrated coatings as a result of exposure to microgrowths, to quantify their effect on changes in physics-mechanical, tribotechnical and other (wetting, adhesion, etc.) properties, to perform a comparative analysis of the microrelief and nanotexture transformations of the initial and the fluorinated polymer materials. From a strategic perspective, we will expand the list of microorganisms for which new studies on biostability will be carried out, and we will also study the effect of the fluorine content in the modifying gas mixture, the duration and mode of modification on the structure and properties of the already considered and other polymer materials.

Author Contributions: Conceptualization, F.D.; Methodology, G.R. and Y.R.; Software, Y.R.; Validation, A.E.; Resources, A.E. and M.S.; Writing—original draft, F.D. and V.N.; Writing—review & editing, F.D. and G.R.; Visualization, M.S.; Project administration, V.N.; Funding acquisition, F.D. All authors have read and agreed to the published version of the manuscript.

Funding: The reported study was funded by Moscow Polytechnic University (Grant named after V. E. Fortov).

Institutional Review Board Statement: Not applicable.

Informed Consent Statement: Not applicable.

Data Availability Statement: Not applicable.

Conflicts of Interest: The authors declare no conflict of interest.

References

1. Yang, H.E.; Bruckman, L.S.; French, R.H. *Durability and Reliability of Polymers and Other Materials in Photovoltaic Modules*; Elsevier: Amsterdam, The Netherlands, 2019; pp. 1–342. [CrossRef]
2. Banerjee, I.; Pangule, R.C.; Kane, R.S. Antifouling coatings: Recent developments in the design of surfaces that prevent fouling by proteins, bacteria, and marine organisms. *Adv. Mater.* **2011**, *23*, 690–718. [CrossRef] [PubMed]
3. Bustamante-Torres, M.; Arcentales-Vera, B.; Estrella-Nuñez, J.; Yánez-Vega, H.; Bucio, E. Antimicrobial Activity of Composites-Based on Biopolymers. *Macromol* **2022**, *2*, 258–283. [CrossRef]
4. Qiu, H.; Si, Z.; Luo, Y.; Feng, P.; Wu, X.; Hou, W.; Huang, D. The Mechanisms and the Applications of Antibacterial Polymers in Surface Modification on Medical Devices. *Front. Bioeng. Biotechnol.* **2020**, *8*, 910. [CrossRef] [PubMed]
5. Alamri, A.; El-Newehy, M.H.; Al-Deyab, S.S. Biocidal polymers: Synthesis and antimicrobial properties of benzaldehyde derivatives immobilized onto amine-terminated polyacrylonitrile. *Chem. Cent. J.* **2012**, *6*, 111. [CrossRef] [PubMed]
6. El-Newehy, M.H.; Meera, M.A.; Aldalbahi, A.K.; Thamer, B.M.; Mahmoud, Y.A.G.; El-Hamshary, H. Biocidal polymers: Synthesis, characterization and antimicrobial activity of bis-quaternary onium salts of poly(aspartate-co-succinimide). *Polymers* **2021**, *13*, 23. [CrossRef]
7. Siedenbiedel, F.; Tiller, J.C. Antimicrobial polymers in solution and on surfaces: Overview and functional principles. *Polymers* **2012**, *4*, 46–71. [CrossRef]
8. Gerba, C.P. Quaternary ammonium biocides: Efficacy in application. In *Applied and Environmental Microbiology*; American Society for Microbiology: Washington, DC, USA, 2015. [CrossRef]
9. Chen, Z.; Wang, Q.; Zhang, Z.; Lei, H. Preparation and properties of antibacterial fluorinated acrylic emulsion. *React. Funct. Polym.* **2021**, *163*, 104901. [CrossRef]
10. Irshad, K.; Rehman, K.; Sharif, H.; Akash, M.S.H. Antimicrobial Polymer Coating. In *Polymer Coatings*; Wiley: Hoboken, NJ, USA, 2020; pp. 347–358. [CrossRef]
11. Pinho, A.C.; Piedade, A.P. Polymeric coatings with antimicrobial activity: A short review. *Polymers* **2020**, *12*, 2469. [CrossRef]
12. Sasi, R.; Sreejith, S.L.; Ramesh, G.; Sherin, D.R.; Kaviyil, J.E.; Paul, W.; Joseph, R. Ionic liquid based antimicrobial coating on polymeric surface: A green chemistry approach. *Results Surf. Interfaces* **2021**, *5*, 100026. [CrossRef]
13. Nazarov, V.G.; Stolyarov, V.P.; Gagarin, M.V. Simulation of chemical modification of polymer surface. *J. Fluor. Chem.* **2014**, *161*, 120–127. [CrossRef]

14. Zhang, X.; Wang, L.; Levänen, E. Superhydrophobic surfaces for the reduction of bacterial adhesion. *RSC Adv.* **2013**, *3*, 12003–12020. [CrossRef]
15. Prorokova, N.P.; Istratkin, V.A.; Kumeeva, T.Y.; Vavilova, S.Y.; Kharitonov, A.P.; Bouznik, V.M. Improvement of polypropylene nonwoven fabric antibacterial properties by the direct fluorination. *RSC Adv.* **2015**, *5*, 44545–44549. [CrossRef]
16. Kharitonov, A.P. Direct fluorination of polymers-From fundamental research to industrial applications. *Prog. Org. Coat.* **2008**, *61*, 192–204. [CrossRef]
17. Nazarov, V.G.; Doronin, F.A.; Evdokimov, A.G.; Rytikov, G.O.; Stolyarov, V.P. Oxyfluorination-Controlled Variations in the Wettability of Polymer Film Surfaces. *Colloid J.* **2019**, *81*, 146–157. [CrossRef]
18. Nazarov, V.G.; Stolyarov, V.P.; Doronin, F.A.; Evdokimov, A.G.; Rytikov, G.O.; Brevnov, P.N.; Zabolotnov, A.S.; Novokshonova, L.A.; Berlin, A.A. Comparison of the Effects of Some Modification Methods on the Characteristics of Ultrahigh-Molecular-Weight Polyethylene and Composites on Its Basis. *Polym. Sci.-Ser. A.* **2019**, *61*, 325–333. [CrossRef]
19. Doronin, F.A.; Rudyak, Y.V.; Rytikov, G.O.; Evdokimov, A.G.; Nazarov, V.G. 3D-printed planar microfluidic device on oxyfluorinated PET-substrate. *Polym. Test.* **2021**, *99*, 107209. [CrossRef]
20. Nazarov, V.G.; Nagornova, I.V.; Stolyarov, V.P.; Doronin, F.A.; Evdokimov, A.G.; Brevnov, P.N.; Zabolotnov, A.S.; Novokshonova, L.A. Effect of Fluorination of Ultrahigh-Molecular-Weight Polyethylene and Its Composites on the Surface Structure and Properties. Russ. *J. Phys. Chem. B.* **2018**, *12*, 1066–1075. [CrossRef]
21. Rytikov, G.O.; Doronin, F.A.; Evdokimov, A.G.; Rudyak, Y.V.; Nazarov, V.G. The Effect of Morphological Surface Inhomogeneities on the Mycological Resistance of Polymer Films. *Prot. Met. Phys. Chem. Surf.* **2021**, *57*, 422–431. [CrossRef]
22. Chug, M.K.; Brisbois, E.J. Recent Developments in Multifunctional Antimicrobial Surfaces and Applications toward Advanced Nitric Oxide-Based Biomaterials. *ACS Mater. Au* **2022**, *2*, 525–551. [CrossRef]
23. Stewart, A.; Finer, Y. Biostable, antidegradative and antimicrobial restorative systems based on host-biomaterials and microbial interactions. *Dent. Mater.* **2019**, *35*, 36–52. [CrossRef]
24. Taunk, A.; Chen, R.; Iskander, G.; Ho, K.K.K.; Black, D.S.C.; Willcox, M.D.P.; Kumar, N. Dual-Action Biomaterial Surfaces with Quorum Sensing Inhibitor and Nitric Oxide to Reduce Bacterial Colonization. *ACS Biomater. Sci. Eng.* **2018**, *4*, 4174–4182. [CrossRef] [PubMed]
25. Kharitonov, A.P.; Simbirtseva, G.V.; Bouznik, V.M.; Chepezubov, M.G.; Dubois, M.; Guérin, K.; Hamwi, A.; Kharbache, H.; Masin, F. Modification of ultra-high-molecular weight polyethylene by various fluorinating routes. *J. Polym. Sci. Part A Polym. Chem.* **2011**, *49*, 3559–3573. [CrossRef]
26. Doronin, F.A.; Rytikov, G.O.; Evdokimov, A.G.; Ruduak, Y.V.; Nazarov, V.G. The synergistic effect of bulk-surface modification onto the wear resistance of the ultrahigh molecular weight polyethylene. *Polym. Polym. Compos.* **2023**, *31*. [CrossRef]
27. Doronin, F.A.; Savelev, M.A.; Taranets, I.P.; Rudyak, Y.V.; Rytikov, G.O.; Nazarov, V.G. The variation-rotational anisotropy aproach to the polymer based materials surface morphological heterogeneity. *Russ. J. Gen. Chem.* **2021**, *65*, 8–15. [CrossRef]
28. Doronin, F.A.; Evdokimov, A.G.; Rudyak, Y.V.; Rytikov, G.O.; Taranets, I.P.; Nazarov, V.G. A new approach to function-structure modeling of the surface modified polymers. *Nanosyst. Phys. Chem. Math.* **2022**, *13*, 115–127. [CrossRef]
29. Tressaud, A.; Durand, E.; Labruge, C.; Kharitonov, A.P.; Simbirtseva, G.V.; Kharitonova, L.N.; Dubois, M. Surface modification of polymers treated by various fluorinating media. *Acta Chim. Slov.* **2013**, *60*, 495–504.

Disclaimer/Publisher's Note: The statements, opinions and data contained in all publications are solely those of the individual author(s) and contributor(s) and not of MDPI and/or the editor(s). MDPI and/or the editor(s) disclaim responsibility for any injury to people or property resulting from any ideas, methods, instructions or products referred to in the content.